FATIGUE CRACK PROPAGATION THROUGH RESIDUAL STRESS FIELDS

B. L. Averbach* and Bingzhe Lou**

**Massachusetts Institute of Technology, Cambridge, MA 02139, USA*
***Shanxi Mechanical Institute, Peoples' Republic of China*

ABSTRACT

The propagation of fatigue cracks through carburized cases has been studied in two high alloy steels at a constant stress intensity range (ΔK) and at a constant cyclic peak load. The crack propagation rates (da/dN) were significantly decreased in residual compressive stress fields and increased in tensile stress fields. A superposition model was used to interpret these phenomena. We define an internal stress intensity factor, $K_i = \delta_i d_i^{\frac{1}{2}}$, where δ_i is the residual stress at a given point and d_i is a distance characteristic of the internal stress distribution, and the effective stress intensity becomes, $K_e = K_a + K_i$, where K_a is the applied stress intensity. Values of K_e are interpreted to be equivalent to ΔK_e, the effective cyclic stress intensity factor, and used to predict the crack propagation rates from experimental da/dN vs ΔK curves for the unstressed material. A reasonably good fit was obtained using measured values of δ_i and a value of d_i = 11 mm (.43).

KEYWORDS

Fatigue crack propagation; residual stresses; carburized cases

EXPERIMENTAL

We have investigated the behavior of fatigue cracks progressing through a carburized case into a tougher core in two steels, designated as M-50NiL (.13 C, 4.25 Mo, 4.14 Cr, 1.32 V, 3.49 Ni), and CBS - 1000M (.15 C, 4.49 Mo, 1.05 Cr, 0.39 C, 3.01 Ni). Compact tension specimens 6.1 x 6.35 x 1.3 cm (2.4 x 2.5 x 0.5 in) were selectively carburized as shown in Fig. 1 to a depth of approximately 2.5 mm (0.100) in. in the notch region, with a resultant carbon content of about 1 wt pct at the surface. The maximum hardness was Rc 62 in the case and Rc 46 in the core. After carburizing and heat treating, the specimens were polished and the notch was sharpened by an abrasive string saw which was used to introduce a cut 0.15 mm wide by 1 mm deep. Fatigue cracks were initiated in a servohydraulic tensile machine under load control at 50 Hz at ΔK = 12 - 15 MPa·m$^{\frac{1}{2}}$ (11 - 14 ksi·in$^{\frac{1}{2}}$) and a minimum-to-maximum ratio of ΔK, R = 0.1. Details of the heat treating and test procedures have been reported elsewhere (1,2).

Two types of experiments were run. In the first we propagated the cracks at a constant value of peak load 5960 N (1340 lbs). Base line data of da/dN vs ΔK were obtained for the core materials, using uncarburized heat treated specimens, and for the case materials using through-carburized thinner compact tension specimens, 0.65 mm (0.25 in.) thick.

The base line data, da/dN vs ΔK are shown in Figs. 2 and 3. The properties of the case are very close to those of the standard bearing steel, M-50 (.84 C, 4.20 Mo, 4.30 Cr, 1.00 V), and these values of da/dN are included for comparison.

The crack propagation rates through the carburized M-50NiL and CBS-1000M at ΔK = 17MPa·m$^{\frac{1}{2}}$ are shown in Fig. 4. At this value of ΔK, the case is in the rapid fracture regime, but we see that the propagation rate is slowed significantly in M-50NiL as the crack passes through the carburized region. Beyond the carburized zone, at about 3 mm from the surface, the propagation rates are those expected for the core material. The situation

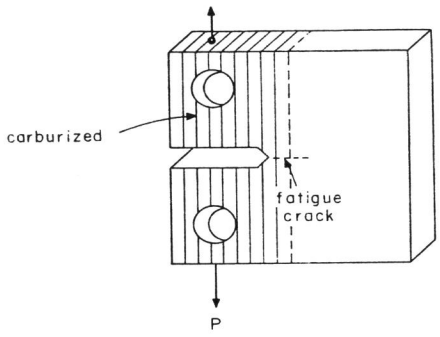

Figure 1. Carburized compact tension specimens.

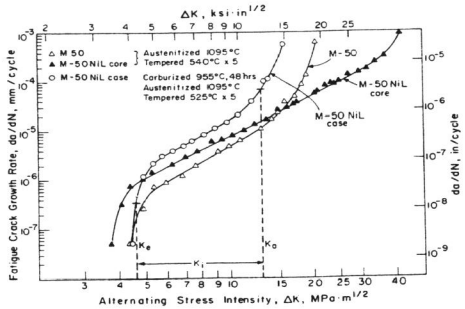

Figure 2. Fatigue crack propagation rates in M-50NiL case and core materials. The effects of an internal stress intensity, K_i, corresponding to a residual compressive stress are also indicated.

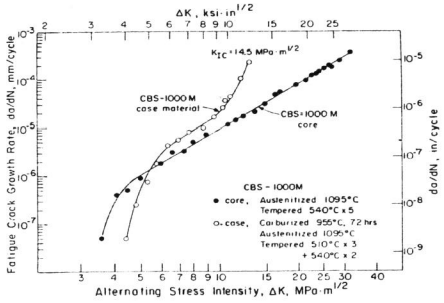

Figure 3, Fatigue crack growth propagation rates in CBS-1000M case and core material.

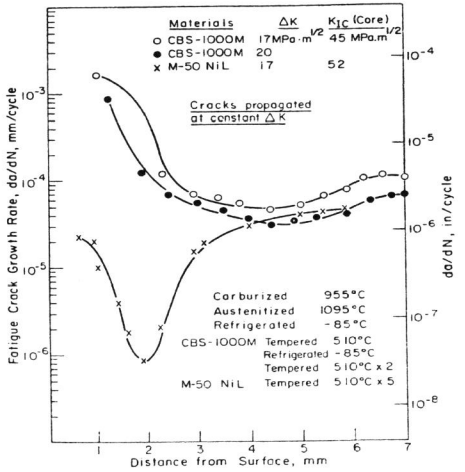

Figure 4. Fatigue crack propagation through carburized cases in CBS-1000M and M-50NiL at constant values of ΔK.

is different in CBS-1000M. The crack rate in the case is different in CBS-1000M. The crack rate in the case is higher than that expected for the case material, but da/dN also approaches the rate expected for the core at a depth of 3 mm.

Crack propagation rates at a constant cyclic peak load are shown in Figs. 5 and 6. In M-50NiL (Fig. 5), the fatigue crack-propagation rate fell sharply in the case and stopped at $\Delta K = 13\ MPa \cdot m^{\frac{1}{2}}$. It was reinitiated by raising the load slightly and the crack propagation was then continued at the original load. In CBS-1000M (Fig.6) the crack slowed somewhat in the case, but the effect was not as pronounced as in M-50NiL.

Residual stresses were measured as a function of depth by an X-ray method and these are shown in Figs. 7 and 8. It is evident that residual compressive stresses were developed in the case of M-50NiL, but that the stresses in the case of CBS-1000M were predominately tensile.

DISCUSSION

It is apparent that the fatigue crack propagation rates have been affected by the residual stresses and we consider a model to describe these efforts. Nelson (3) has used a superposition model wherein a stress intensity, K_i, is used to account for the effects of residual stress, and the resultant effective stress intensity becomes $K_e = K_a + K_i$, where K_a is the externally applied stress intensity factor. Closure models were used to calculate K_i, but the values for the geometry used here have not been calculated. Parker(4) has used another approach, defining an effective value of the stress intensity ratio, $R_e = K_e(min)/K_e(max)$, but this requires values of da/dN for various values of R, and these data are not usually available. Elber (5) has also used a superposition method for surface fatigue cracks propagating through shot-peened sheets and shown that K_i was negative for a depth extending just beyond the compression zone, and positive thereafter. Harris and Tetelman (6) also used a superposition model to describe crack propagation in a specimen to which side compressive load were used to arrest a propagating crack. In the closure model used by Kim et al (7)

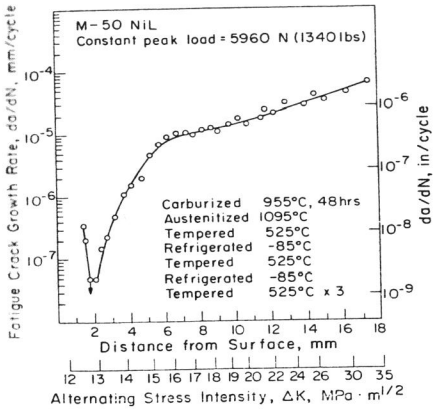

Figure 5. Fatigue crack propagation through carburized M-50NiL at a cyclic load with a constant peak value, 5960 N (1340 lbs).

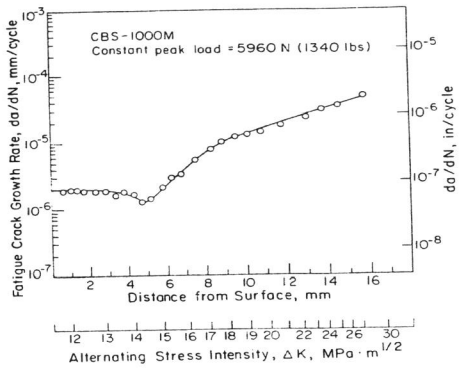

Figure 6. Fatigue crack propagation through carburized CBS-1000M at a cyclic load with a constant peak value, 5960 N, (1340 lbs).

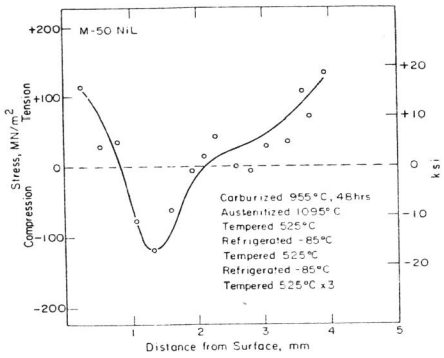

Figure 7. Residual stresses in carburized M-50NiL.

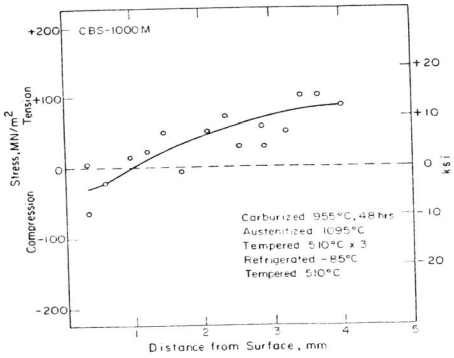

Figure 8. Residual stresses in carburized CBS-1000M.

it was assumed that the residual stresses act perpendicularly to the surfaces of the crack and that only the residual stresses acting across the crack face can influence the stress intensity. The residual stresses in the carburized case are biaxial in planes normal to the direction of crack propagation, thus introducing crack closure and crack arrest features in a complex stress system. In our model we have used the superposition approach and associated the internal stresses with an internal stress intensity factor, K_i, which is added to the applied stress intensity factor, K_a. Thus the net or effective stress intensity, K_e, becomes:

$$K_e = K_a + K_i \qquad (1)$$

where, K_e = the effective stress intensity factor

K_a = the applied stress intensity factor, calculated from the applied load P, the crack length, and the specimen geometry

K_i = the stress intensity factor introduced by other factors such as internal stress, side loads, etc.

We have visualized the internal stress intensity as arising from the residual stresses in the unbroken ligament, in analogy with the application of a side load as in the Harris and Tetelman treatment (6). We assume that the internal stress intensity in a given region is given by:

$$K_i = \delta_i d_i^{\frac{1}{2}} \qquad (2)$$

where, δ_i = internal stress normal to the direction of crack propagation

d_i = distance characteristic of the pattern of internal stress distribution

In carburized cases, δ_i, arises from thermal effects of phase transformations in the case and core, and we suggest that d_i is associated with the depth of the region which is carburized. In these specimens, carbon has been added to a depth of about 5-6 mm, and we assume that the corresponding residual stress patterns extend for a distance of about 11 mm. We thus have

a clothespin, Fig. 9, with an internal stress system σ_i, just ahead of the notch, and extending over a distance, d_i = 11 mm (.43 in). This is a simplified version of the side-load geometry used by Harris and Tetelman.

We applied equation (2) using the residual stress pattern shown in Figs. 7 and 8 for carburized M-50NiL and CBS-1000M and calculated values of K_i as a function of distance from the surface. In our convention, compressive stresses are negative and thus result in negative values of K_i. We then calculated the values of the effective stress intensity factors, K_e, as a function of distance from the surface, using K_a = 17 MPa·m$^{\frac{1}{2}}$ (15.5ksi·in$^{\frac{1}{2}}$) to correspond to the test run at a constant ΔK_a in fatigue crack propagation, we determined the corresponding value of the crack propagation rate, da/dN, from the experimental curves given in Figs. 2 and 3. For the first 1.5 mm of the case, where the carbon level was about 1 pct, the da/dN curve for the completely carburized case was used. From 1.5 to 2 mm, the curve for M-50 was used, and beyond that, the curve for the core was judged to be most representative of the structure. The calculated curves of da/dN are shown in Figs. 10 and 11 as a function of the distance from the peak load and the measured crack lengths, and K_i was calculated from the residual stress patterns as indicated. The effect of a residual stress of 90 MNm^{-2} (13ksi) in compression on a crack with an applied stress intensity, K_a = 13 MPa·m$^{\frac{1}{2}}$, is shown schematically in Fig. 1. Comparisons with the observed values of da/dN are also shown in Fig. 10 and 11.

The agreement with the observed values is good in that we have reproduced the shapes of the curves for the tests at ΔK = 17 MPa·m$^{\frac{1}{2}}$, and at constant peak load, quite well. The minima of the calculated curves are displaced, and this disparity is influenced by two factors. The residual stress pattern in the notch was not determined directly; it was inferred from data which were taken from a flat surface which was carburized at the same time. The location of the maximum compressive stress in

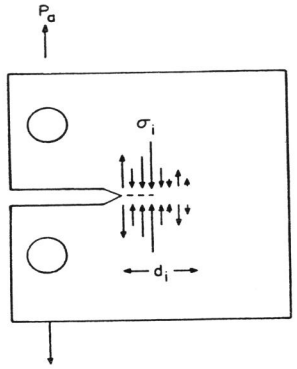

$$K_i = \sigma_i d_i^{1/2}$$

$$K_e = K_a + K_i$$

Figure 9. Internal clothespin model for effects of internal stresses on the rates of fatigue crack propagation.

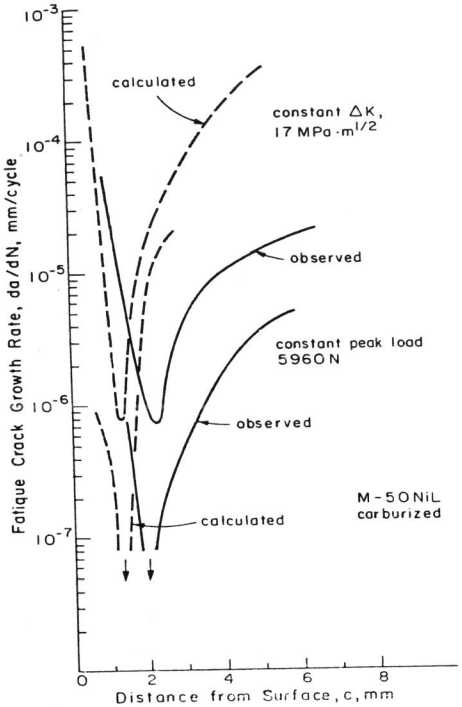

Figure 10. Calculated and observed values of da/dN in carburized M-50NiL.

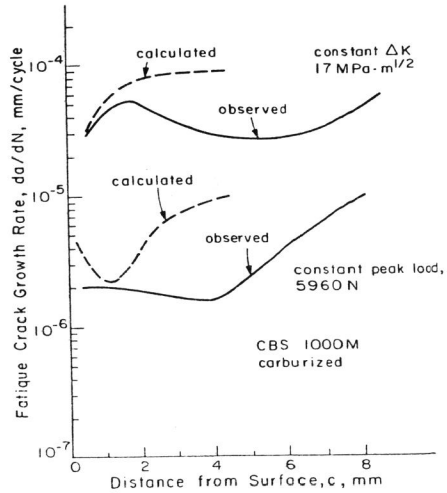

Figure 11. Calculated and observed value of da/dN in carburized CBS-1000M steel.

the notch could thus have been somewhat different. But also, we have not taken into account the redistribution of residual stresses which takes place as the crack propagates through the residual stress zone. It is probable that the compressive residual stresses are pushed deeper into the specimen as the crack propagates. For this reason, we have matched the calculated fatigue crack growth rates only for distances which are small relative to the case depth, since redistribution of stresses would certainly affect the validity of the calculation at greater depths.

CONCLUSIONS

Our data indicate that it is possible to carburize a modified high-speed steel (M-50NiL) to produce a combination of a hard case and a tough core which can slow, and even stop, propagating fatigue cracks. Considerable benefits are achieved by inducing residual compressive stresses in the case. On the other hand, tensile stresses are induced in the case on carburizing CBS-1000M, and fatigue cracks are accelerated under these conditions.

The effects of residual stresses on the fatigue crack propagation rates are qualitatively predicted by an internal clothespin model wherein the effects of residual stresses are introduced in terms of an internal stress intensity factor, $K_i = \sigma_i d_i^{\frac{1}{2}}$, where σ_i is the internal stress and d_i the effective distance over which the internal stress acts. The net effective stress intensity factor, $K_e = K_a + K_i$, is reduced when the internal stresses are compressive (i.e. when σ_i is negative) and a corresponding reduction in the fatigue crack propagation rate is observed. We have assumed that d_i is approximately equal to twice the total carburation depth, (i.e., d_i = 11 mm; 0.43 in), and this appears to provide reasonably good agreement with the observed values of the crack propagation rates. We emphasize that the model is only qualitative since the redistribution of stress in front of the advancing fatigue crack has not been taken into account.

ACKNOWLEDGEMENTS

The authors would like to acknowledge the sponsorship of the U.S. Air Force and the U.S. Navy Air Propulsion Center and the encouragement we have received from Dr. James F. Dill of AFWAL/POSL. We would also like to acknowledge the substantial assistance which we have received from the Fafnir Bearing Division of Textron, Inc., and the General Electric Company Aircraft Bearing Engine Group. The authors would also like to acknowledge the very able assistance of Robert E. Denison of Fafnir in making our experimental measurements and also several interesting discussions with John C. Clark of General Electric.

REFERENCES

1. Averbach, B.L., Bingzhe Lou, P.K. Pearson, R.E. Fairchild, and E.M. Bamberger. "Fatigue Crack Propagation in Carburized High Alloy Bearing Steels." (in press).
2. Averbach, B.L. (1980). Metal Progress, 118, 19.
3. Nelson, D.V. (1982). in Residual Stress Effects in Fatigue, ASTM STP 776, American Society for Testing and Materials, pp. 172-194.
4. Parker, A.P. (1982). in Residual Stress Effects in Fatigue, ASTM STP 776, American Society for Testing and Materials, pp. 13-31.
5. Elber, W. (1982). in Fracture Toughness and Slow Stable Cracking, ASTM STP 776, American Society for Testing and Materials, pp. 224-234.
6. Harris, D.O. and A.S. Tetelman (1972). Eng Fracture Mech., 4, p. 93.
7. Kim, C., D.E. Diesburg, and G.T. Eldis (1982). in Residual Stress Effects in Fatigue, ASTM STP 776, American Society for Testing and Materials, pp. 224-234.